AFRL-RY-RS-TR-2010-064
Final Technical Report
March 2010

MODULATION DIVERSITY IN WAVEFORM DESIGN

Syracuse University

AIR FORCE RESEARCH LABORATORY
SENSORS DIRECTORATE
ROME RESEARCH SITE
ROME, NEW YORK

NOTICE AND SIGNATURE PAGE

Using Government drawings, specifications, or other data included in this document for any purpose other than Government procurement does not in any way obligate the U.S. Government. The fact that the Government formulated or supplied the drawings, specifications, or other data does not license the holder or any other person or corporation; or convey any rights or permission to manufacture, use, or sell any patented invention that may relate to them.

This report was cleared for public release by the 88th ABW, Wright-Patterson AFB Public Affairs Office and is available to the general public, including foreign nationals. Copies may be obtained from the Defense Technical Information Center (DTIC) (http://www.dtic.mil).

AFRL-RY-RS-TR-2010-064 HAS BEEN REVIEWED AND IS APPROVED FOR PUBLICATION IN ACCORDANCE WITH ASSIGNED DISTRIBUTION STATEMENT.

FOR THE DIRECTOR:

/s/
JEFFREY T. CARLO
Work Unit Manager

/s/
DENNIS BIRCHENOUGH, Deputy Chief
RF Sensor Technology Division
Sensors Directorate

This report is published in the interest of scientific and technical information exchange, and its publication does not constitute the Government's approval or disapproval of its ideas or findings.

REPORT DOCUMENTATION PAGE

Form Approved
OMB No. 0704-0188

1. REPORT DATE *(DD-MM-YYYY)*	2. REPORT TYPE	3. DATES COVERED *(From - To)*
MARCH 2010	Final	August 2004 – August 2009

4. TITLE AND SUBTITLE

MODULATION DIVERSITY IN WAVEFORM DESIGN

5a. CONTRACT NUMBER
N/A

5b. GRANT NUMBER
FA8750-04-1-0283

5c. PROGRAM ELEMENT NUMBER
61102F

6. AUTHOR(S)

Tapan K. Sarkar and Jie Yang

5d. PROJECT NUMBER
WADS

5e. TASK NUMBER
15

5f. WORK UNIT NUMBER
01

7. PERFORMING ORGANIZATION NAME(S) AND ADDRESS(ES)

Syracuse University
113 Bowne Hall
Syracuse, NY 13244-1200

8. PERFORMING ORGANIZATION REPORT NUMBER
N/A

9. SPONSORING/MONITORING AGENCY NAME(S) AND ADDRESS(ES)

AFRL/RYRD
26 Electronic Parkway
Rome NY 13441-4514

10. SPONSOR/MONITOR'S ACRONYM(S)
N/A

11. SPONSORING/MONITORING AGENCY REPORT NUMBER
AFRL-RY-RS-TR-2010-064

12. DISTRIBUTION AVAILABILITY STATEMENT
APPROVED FOR PUBLIC RELEASE; DISTRIBUTION UNLIMITED. PA# RY-2010-0853 Date Cleared: 11-February-2010

13. SUPPLEMENTARY NOTES

14. ABSTRACT
The goal of the research has been to develop and demonstrate spatially and temporally adaptive radio frequency (RF) sensor technology for application to air, space and ground systems operating in isolation or in concert with other sensor systems. The objective has been to be aware of the environment as it is critical to the process of spatial and temporal diversity via both transmit and receive. The idea here is to use the environment as part of the RF sensor system, thereby improving the transmission and reception efficiency. Improved target (air to ground) detection will be achieved under this effort. So not only polarization but also integration of the surrounding environment including the platform is used to optimize the performance for different radar configurations and geometries. Another aspect of the research had been on the design of waveforms for efficient spatial-temporal adaptively including the focusing of the transmitted energy on the target.

15. SUBJECT TERMS
Modulation Diversity, Waveform Design, EM Modeling

16. SECURITY CLASSIFICATION OF:			17. LIMITATION OF ABSTRACT	18. NUMBER OF PAGES	19a. NAME OF RESPONSIBLE PERSON
a. REPORT	b. ABSTRACT	c. THIS PAGE			Jeffrey T. Carlo
U	U	U	UU	32	19b. TELEPHONE NUMBER (*Include area code*) N/A

Table of Contents

LIST OF FIGURES

1.0 SUMMARY

The goal of the research has been to develop and demonstrate spatially and temporally adaptive radio frequency (RF) sensor technology for application to air, space and ground systems operating in isolation or in concert with other sensor systems. The objective has been to be aware of the environment as it is critical to the process of spatial and temporal diversity via both transmit and receive. The idea here is to use the environment as part of the RF sensor system, thereby improving the transmission and reception efficiency. Improved target (air and ground) detection will be achieved under this effort. So not only polarization but also integration of the surrounding environment including the platform is used to optimize the performance for different radar configurations and geometries. Another aspect of the research had been on the design of waveforms for efficient spatial-temporal adaptivity including the focusing of the transmitted energy on the target.

2.0 INTRODUCTION

This report consists of two parts. The first part deals with waveform design using Modulation diversity. The papers presented in section 4.1 are the culmination of these status reports. Briefly we describe the title and the abstract of each of the 5 papers that were generated from this research. The second part consists of work that has been carried out on the placement of antennas on airborne platforms so as to enable a user to transmit the required waveforms. This work is described in section 4.2.

3.0 METHODS AND ASSUMPTIONS

For radiation to occur waveforms must be applied to antennas. An antenna is a temporal filter. An antenna is also a spatial filter. That is why we apply Maxwell's equations as Maxwell's equation solves this spatio-temporal problem in an essentially exact fashion. This is one of the few equations that has not changed in over 100 years as it went through erosion and corrosion of scientific development. Even the advent of relativity had no effect as it is built into Maxwell's equations. This is the uniqueness of this work as the electromagnetic analysis is merged with the signal analysis problem so to address the performance of the complete system.

4.0 RESULTS AND DISCUSSIONS

4.1. Waveform Design Using Modulation Diversity

The results of the research in waveform design, using modulation diversity, have been documented in five technical papers. The following subsections identify the title, authors, and results contained in each of these papers.

4.1.1. A Novel Doppler-Tolerant Polyphase Codes for Pulse Compression Based on the Hyperbolic Frequency Modulation. Authors: J. Yang and T. K. Sarkar

The conventional polyphase pulse compression codes including the Frank code, P1, P2, P3 and P4 codes suffer severe signal loss in performance under a Doppler environment. This paper proposes a new class of polyphase pulse compression codes which are conceptually derived from the step approximation of the phase curve of the hyperbolic frequency modulated chirp signal. By comparing the performance of the conventional codes mentioned earlier and the sidelobe-optimized polyphase P(n,k) code, the peak value of this new polyphase codes degrades much slower in a Doppler environment. In addition, the range estimate as well as the maximum sidelobe levels is almost constant with an increase in the Doppler frequency. The main disadvantage of this polyphase code is the relatively high sidelobe level in the absence of any Doppler effect, and this can be addressed by applying an appropriate window function. The desired Doppler-tolerant property of this new polyphase codes is very attractive for radars employing digital signal processing.

4.1.2. Applying the Fourier-Modified Mellin Transform (FMMT) to Doppler-Distorted Waveforms. Authors: J. Yang, T. K. Sarkar, and P. Antonik

The magnitude spectrum of a time domain signal has the property of delay-invariance. Similar to the delay-invariance property of the Fourier transform, the Mellin transform has the property of scale-invariance. By combining these two transforms together one can form the Fourier-Mellin transform that yields a signal representation which is independent of both delay and scale change. Due to the undesired low-pass property of the Mellin transform (MT), the modified Mellin transform (MMT) which is also scale-invariant is applied in our approach. Therefore the Fourier-Modified Mellin transform (FMMT) of the original signal and the Doppler-distorted signal will be identical. This signal representation is useful in signal detection and target recognition. Several examples dealing with different waveforms have been simulated to illustrate the applicability of this approach. The performance of the Fourier-Modified Mellin transform under different levels of noise in the signal are also illustrated in this paper.

4.1.3. Applying Fourier-Mellin Transform in Doppler-Distorted Waveforms. Authors: Yang and T. K. Sarkar

The magnitude spectrum of a time domain signal has the property of delay-invariance. Similar to that of Fourier transform, Mellin transform has the property of scale- invariance. Combining these two transforms together to form the Fourier-Mellin transform yields a signal presentation which is independent of both delay and scale changes. Therefore the Fourier-Mellin transforms of the original signal and the Doppler-distorted signal will be identical. This signal representation is useful in signal detection and pattern recognition. Several examples dealing with different waveforms have been simulated to illustrate the applicability of this approach.

4.1.4. Acceleration-Invariant Pulse Compression of Hyperbolic Frequency Modulated Waveforms. Authors: J. Yang and T. K. Sarkar

It is well known that hyperbolic frequency modulated waveform is Doppler-invariant. However it suffers severe distortion when the velocity of the target is not constant. In this paper we demonstrate that the acceleration of the target results in a frequency shift which is the source of the signal distortion under the assumption that the acceleration is constant and along the direction of the velocity. Therefore the frequency-shifted version of the matched filter can be applied to eliminate the mismatch between the reflected signal and the matched filter caused by the acceleration of the target. An example of rectangular envelope hyperbolic frequency modulated pulse is presented to illustrate the effect of the acceleration on signal distortion and a bank of filters with selected value of frequency shift are applied to the distorted waveform to improve the compression of the pulse.

4.1.5. Doppler-Invariant Property of Hyperbolic Frequency Modulated Waveforms. Authors: J. Yang and T. K. Sarkar

When the target has large velocity and Doppler effect is not negligible, pulse compression by means of linear frequency modulation suffers from significant signal loss in performance due to the mismatch between the reflected signal and the matched filter caused by the Doppler distortion. This problem can be avoided by using hyperbolic frequency modulated waveform, which has the inherent Doppler-invariant property. In this paper we demonstrate that hyperbolic frequency modulated waveform is Doppler-invariant under the assumption that the target velocity is constant, while linear frequency modulated waveform is not. Two numerical examples with rectangular and Gaussian pulse envelope are presented to compare the performance of these two different modulation schemes under several different levels of Doppler distortion. We also compared the performance of this method with another Doppler-invariant pulse compressor based on bipolar waveform and multiple integrator pair.

4.2. UHF Antenna Design and Analysis

The focus of this section is the design of a UHF antenna to support the radiation of the desired waveforms from a sensor installed on an airborne platform. Unlike the previous section, these results are documented only within this report.

4.2.1. Introduction

The Boeing 737 AEW&C is an Airborne Early Warning & Control aircraft. It was designed in response to Australia's RFP for an aircraft for the Royal Australian Air Force (RAAF) as Project Wedgetail. The aircraft uses the Northrop Grumman Electronic Systems Multi-role Electronically Scanned Array (MESA) radar. The radar is located on a dorsal fin on top of the fuselage, dubbed the "top hat", and is designed for minimal aerodynamic effect. The radar is capable of simultaneous air and sea search, fighter control and area search. [1][2][3][4].
Next we discuss the modeling and the simulation results.

4.2.2. Modeling the Boeing 737 Aircraft

Instead of using a Boeing 737 aircraft, we are going to use a Boeing 767 aircraft in this analysis, and in particular, we have used a 767-200ER for this modeling. [5]

One can find the specifications of a 767-200ER aircraft on the web as described in the next figure. [6]

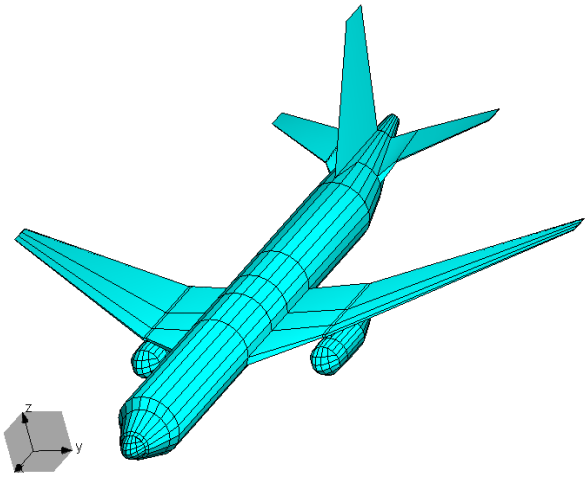

Figure 1. The Electromagnetic Model of the aircraft

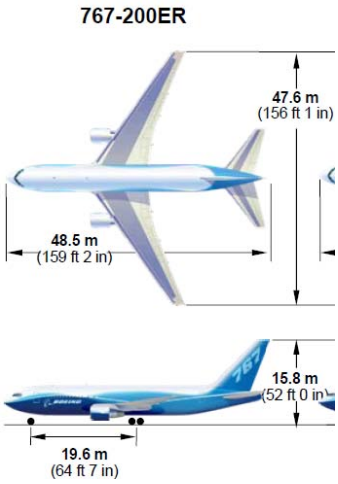

Figure 2. Dimensions of a Boeing 767-200ER aircraft

4.2.3. Electromagnetic Model of the UHF Antenna

From [1][2], we obtained the various dimensions of the Boeing 737 AEW&C aircraft and scaled them accordingly based on the specifications of a Boeing 767-200ER, which one can obtain from the web.

For the specification of the broadside antenna, we chose 9 rows by 11 columns of dipole arrays located on each side. Each of the dipole antenna length is 0.47λ and the spacing between each dipole is 0.5λ. The antenna pattern for this structure is given in Fig 4.

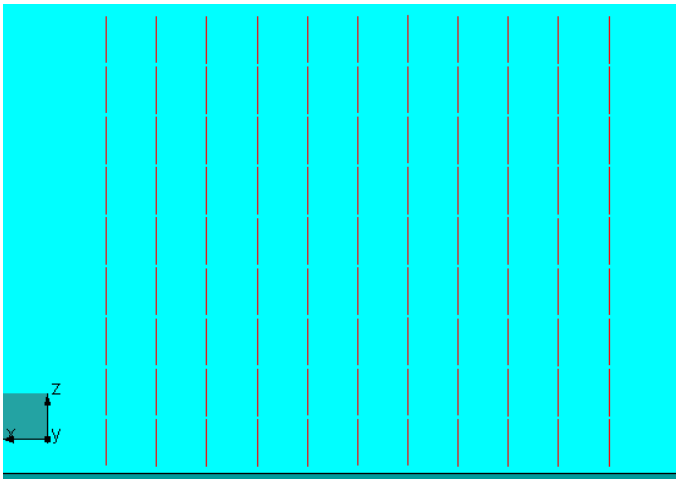

Figure 3. 9 × 11 Dipole Antenna array on both side of the aircraft.

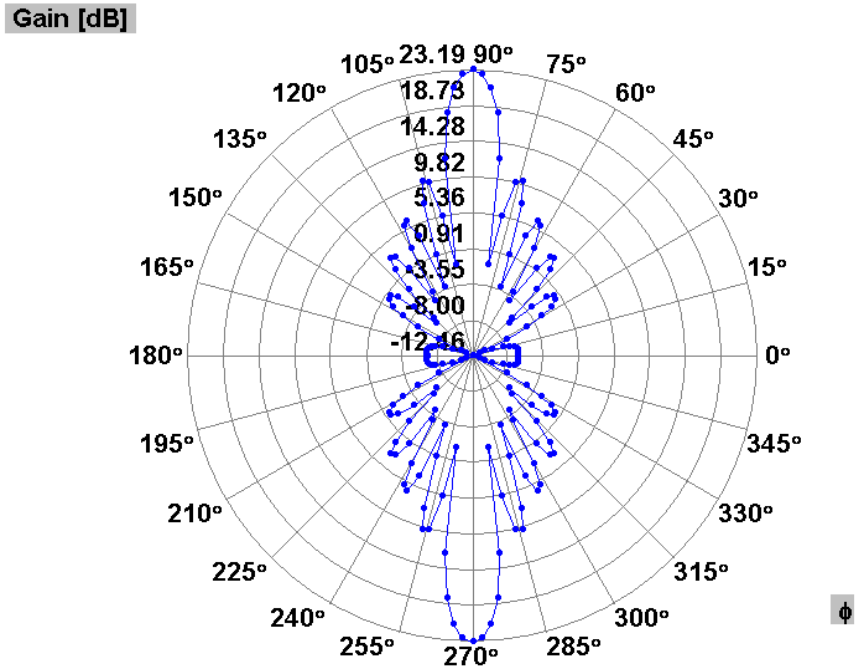

Figure 4. Broadside antenna pattern of the array.

For the front and the back antenna on the aircraft, a 3 element Yagi-Antenna array is used for the front and back sensing. A reflector plate is placed between the front and the back array. The specification for a single Yagi-Antenna is shown below in figures 5 and 6. It has five directors, 1 feeder and 2 reflectors. The dimensions of the length and spacing are based on [7]. The spacing between each element is 0.6λ. The gain of the array is shown in Fig. 7.

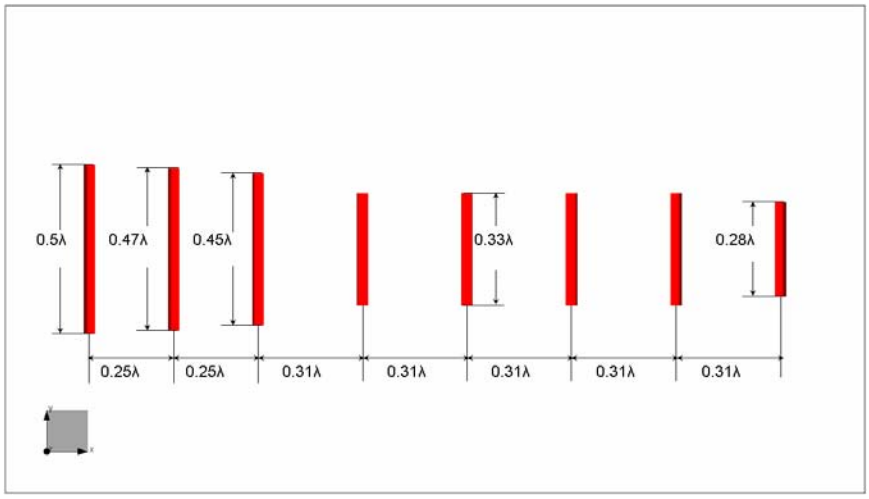

Figure 5. Single element of Yagi Antenna description (5 directors, 1 feeder, and 2 reflectors)

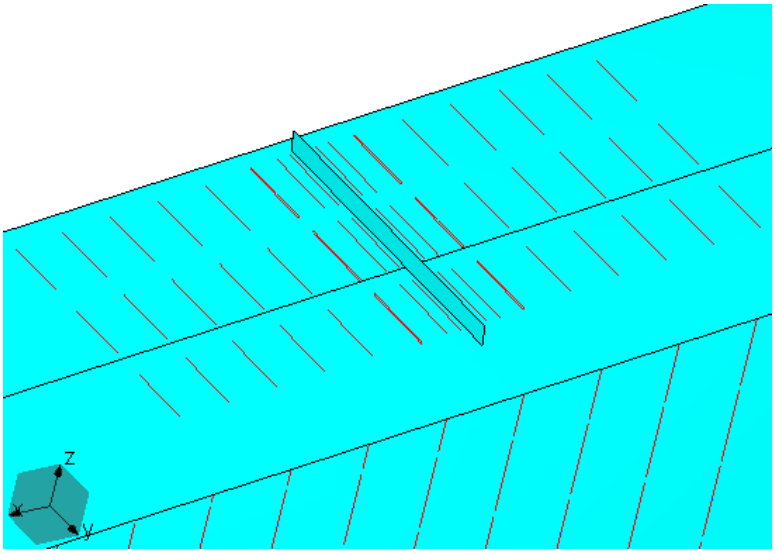

Figure 6. Three Yagi Antennas for the front and the back array.

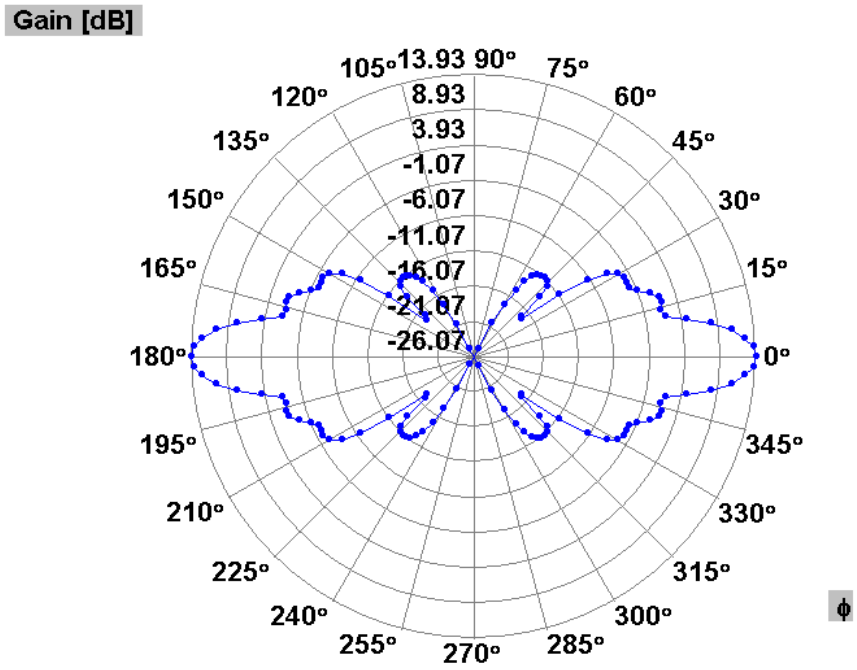

Figure 7. The antenna pattern for the front and the back antenna.

4.2.4. Electromagnetic Model of the Antenna mounted on the Boeing 767-200ER

We now place the antenna array on top of the Boeing aircraft as shown on Fig. 8 called the “top hat”.

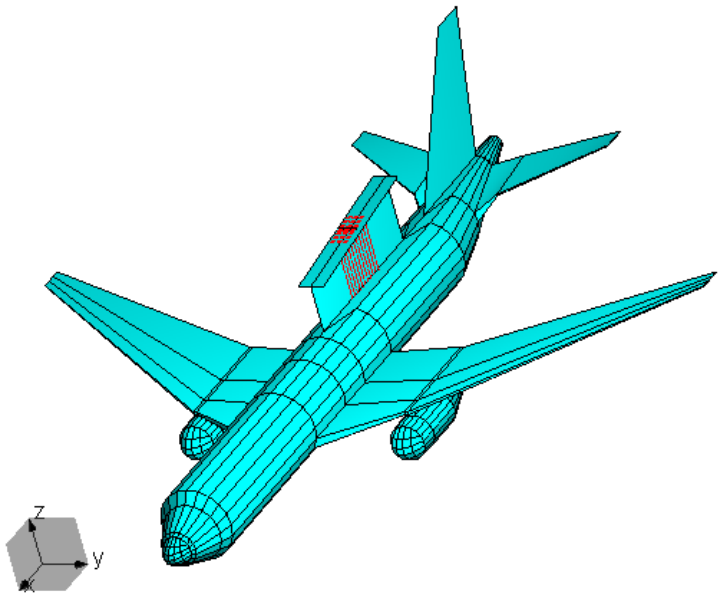

Figure 8. The Boeing 767-200ER with the Antennas.

4.2.5. Electromagnetic Simulations and Results

Fig. 9 plots the azimuth radiation pattern of the antennas along with the platform on which they are mounted, which in this case is the Boeing 767 - 200ER.

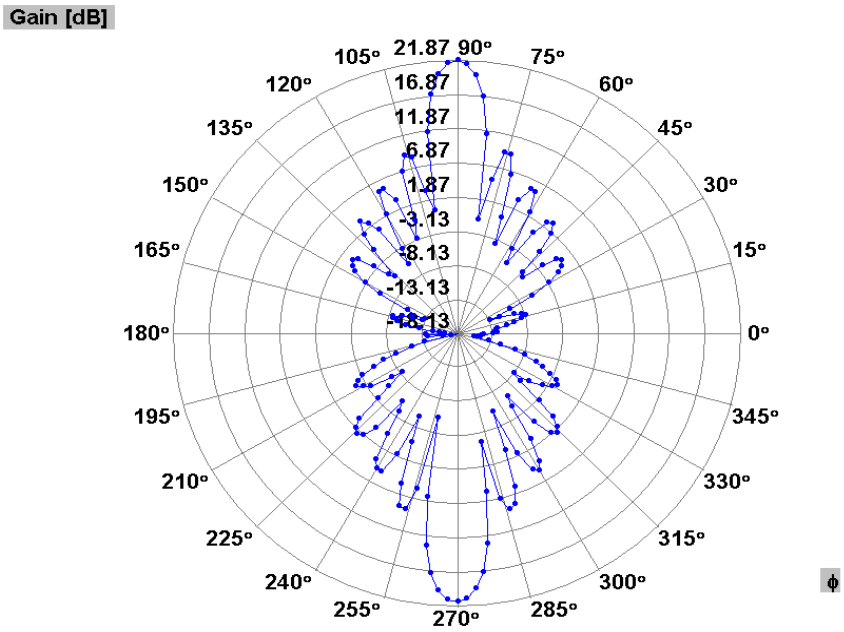

Figure 9. Azimuth Radiation pattern

Because broadside antennas contain more generators than the front and the back antennas, the gain for the front and back is very small. In addition there are some effects of the platform, the Boeing 767-200ER.

The electromagnetic simulator used for the analysis was TIDES (Target IDEntification Software). The total number of unknowns used for this simulation is 94839. The frequency at which the simulations were made is at 400MHz. This numerical simulation took about 303 minutes (about 5 Hours) using the Parallel TIDES codes executed on the CEMLAB Cluster at Syracuse University which consists of 4 nodes, 32cores, CPU speed 2.66 MHz, RAM 2 GB per core, and contain a Giga-bit Ethernet.

4.2.6. Analysis of the UHF Antenna

4.2.6.1. Specifications

The physical dimension of the array is shown in Fig. 10.

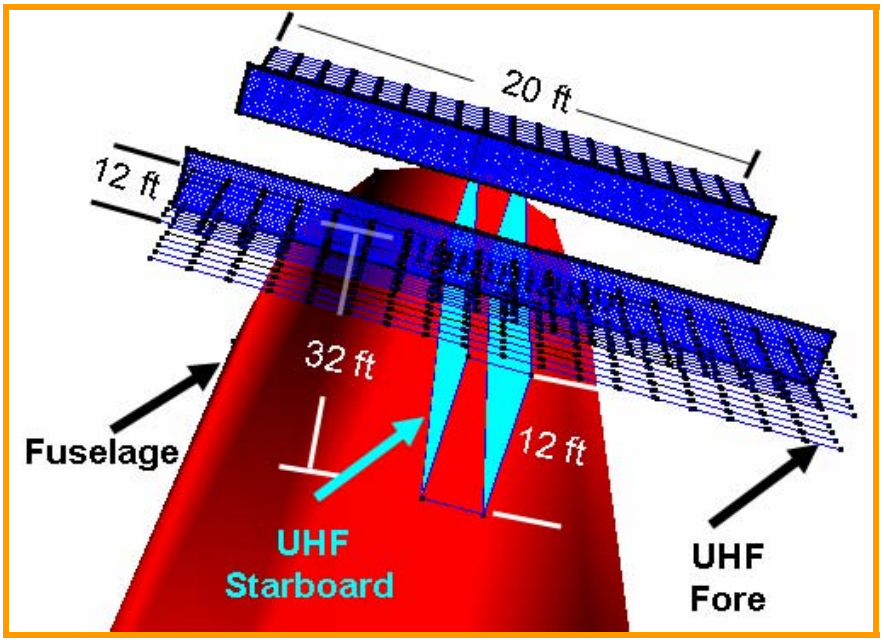

Figure 10. Physical dimensions of the UHF Antenna.

The Fore/Aft Antenna consists of 40 end fire radiators (2 rows by 20 columns) and each element has 10 dipoles end-fire. The size of the antenna is 20 ft by 12 ft (depth) as shown in Fig. 11.

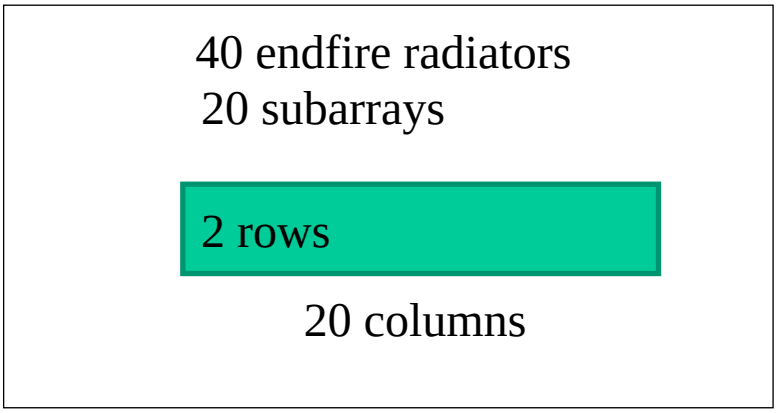

Figure 11. Fore/Aft Antenna Design

The Port/Starboard Antenna consists of 384 dipole elements. (12 rows by 32 columns) and the size of the antenna is 32 ft by 12 ft as shown in Fig. 12.

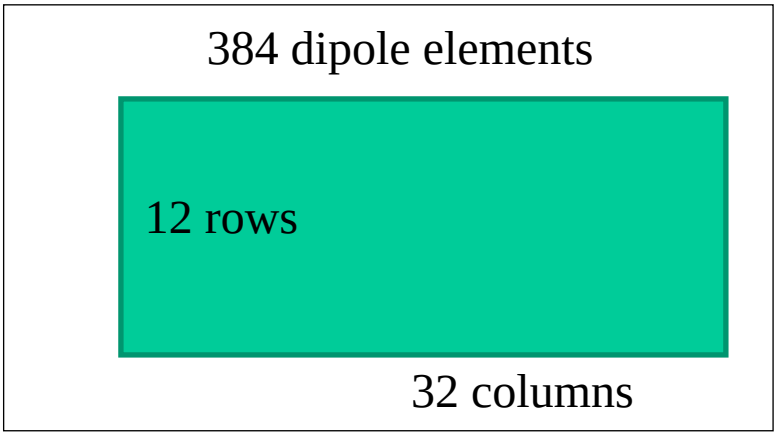

Figure 12. Port/Starboard Antenna Design

4.2.6.2. The TIDES Model for the Antenna

The electromagnetic model consisted of dipoles with a length of 0.47 λ length for all the antennas. The operating frequency is 400 MHz and the spacing between all the elements are half wave length as shown.

Fore/Aft Antenna

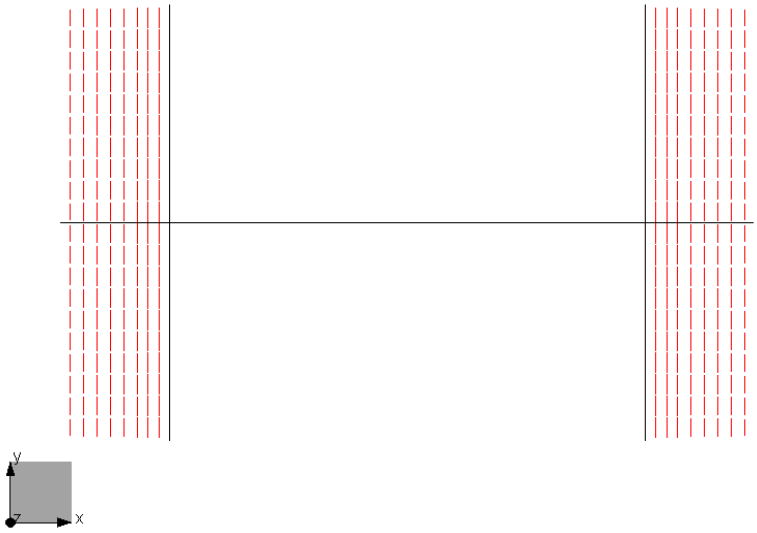

(a) Top view

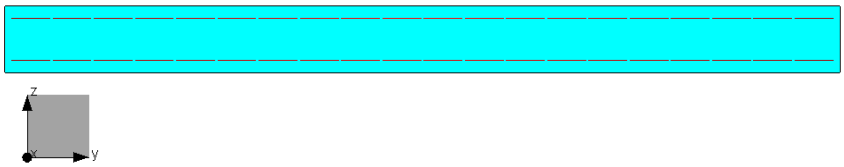

(b) Front view

Figure 13. (a) Top view and (b) Front view of Fore/Aft Antenna

The size of the Fore/Aft antenna model is 11.675 m (38.3 ft) by 1.725 7.6 m (5.66 ft). The spacing between director and feeder is 1/4 λ and between feeder and reflector is also 1/4 λ and between director and director is also 1/4 λ.
The gain of the antenna in the azimuthal plane is plotted in Fig. 14.

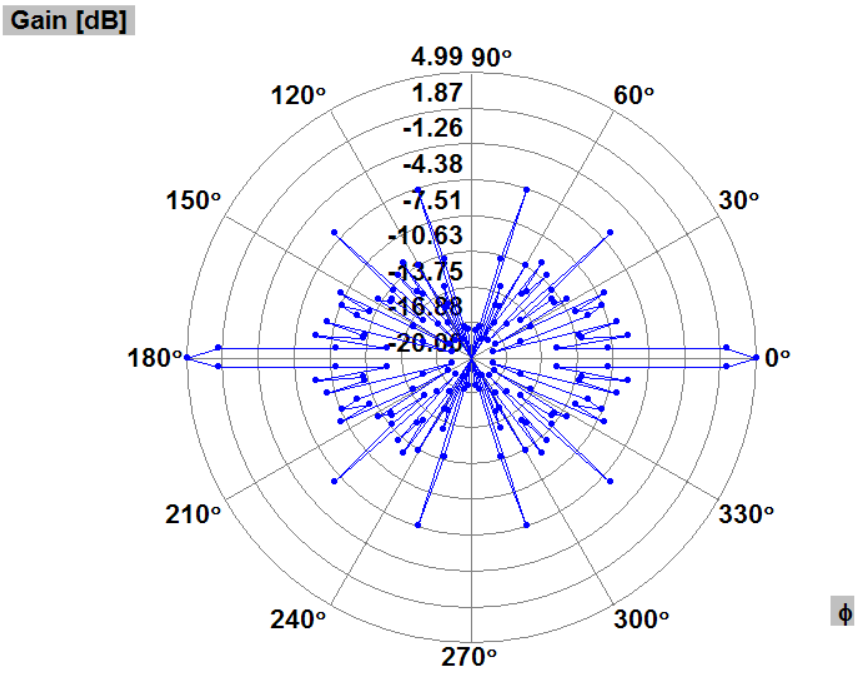

Figure 14. Azimuth Radiation Pattern for Fore/aft Antennas

The size of the Port/Starboard antenna model is 12 m (39.37 ft) by 4.8 m (15.74 ft) as shown In Fig. 15. The gain of the antenna is shown in Fig. 16.

Port/Starboard Antenna

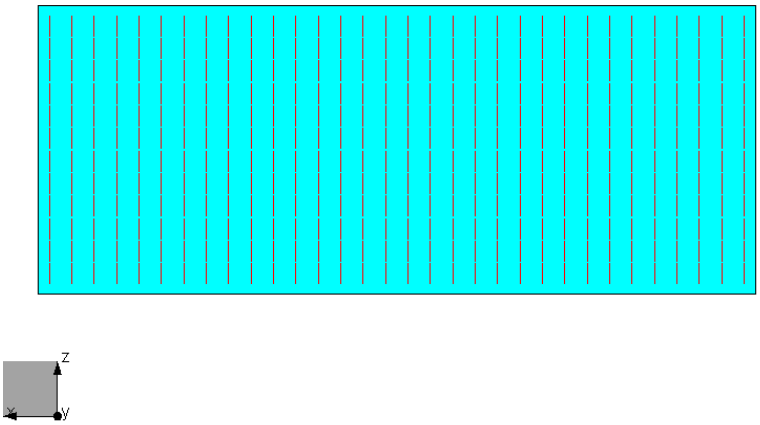

(a) Side view

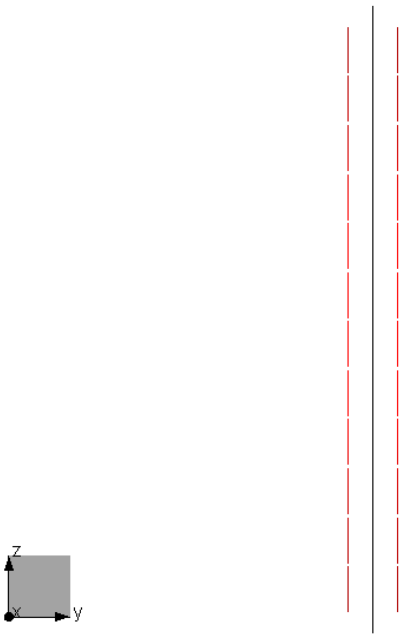

(b) Front view

Figure 15. (a) Side view and (b) Front view of Port/Starboard Antenna

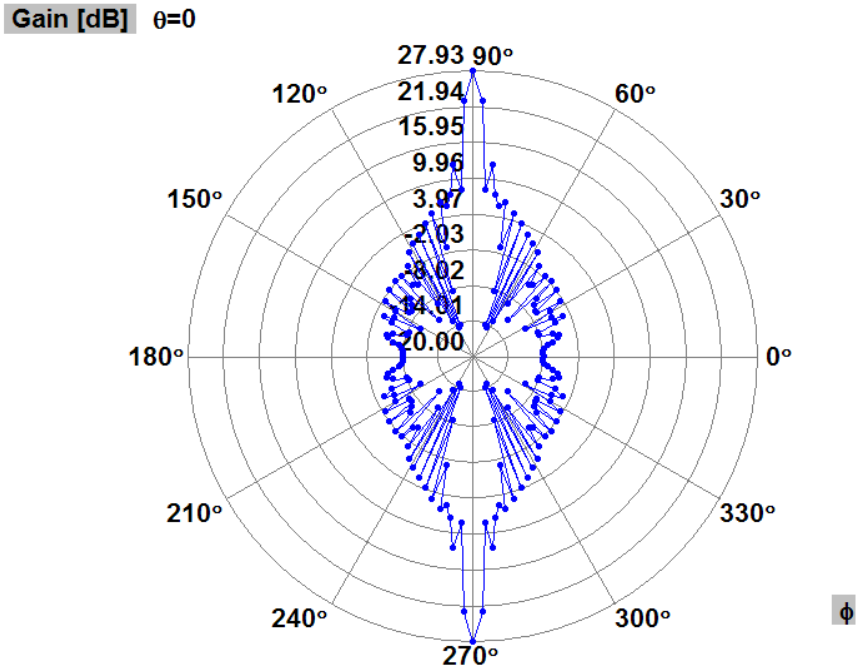

Figure 16. Azimuth Radiation Pattern for Port/starboard Antennas

4.2.6.3. The TIDES Model for the Antenna on the Boeing 767.

The antenna is mounted as the top hat on the Boeing 767-200ER as shown in Fig. 17 along with the dimensions on Fig. 18 .

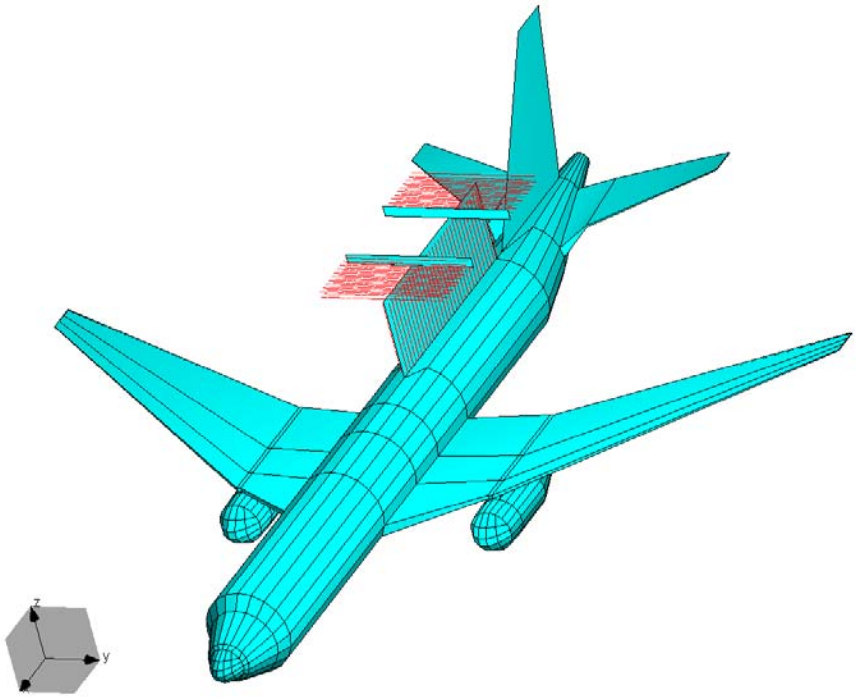

Figure 17. Boeing 767-200ER with Antennas

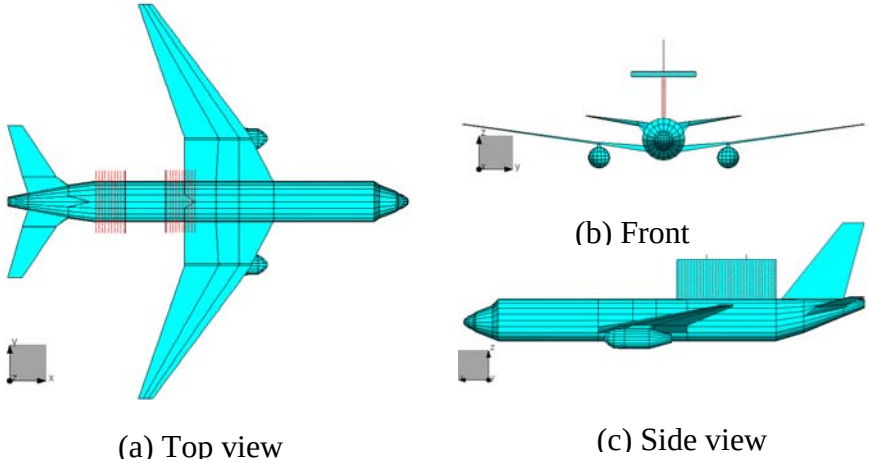

Figure 18. (a) Top view, (b) Front view, and (c) Side view of Boeing 767-200ER along with the Antennas

4.2.6.4. Numerical Simulations and Results

Figure 19 plots the azimuth radiation pattern of the fore/aft and port/starboard antennas in free space and for the Boeing 767 - 200ER with all the antennas installed.

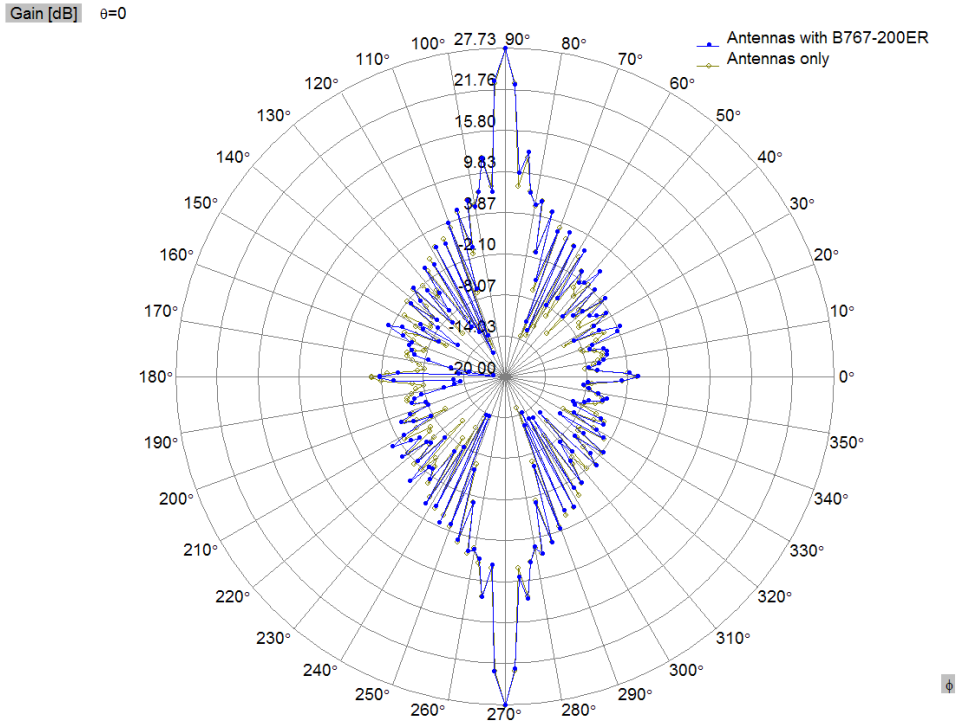

Figure 19. Azimuth Radiation pattern (Blue: Antennas with B767-200ER, Yellow: Antennas only)

To the fore/aft antennas, we have 40 generators on each side and for the port/starboard antennas, we have 384 generators on each side. That's the reason the gain on the port/starboard antennas is greater than on the fore/aft antennas.

The number of unknowns for this simulation is 95939 at 400 MHz. This simulation took about 303 minutes (about 5 Hours) using the Parallel TIDES on the CEMLAB Cluster. (4 nodes, 32cores, CPU speed 2.66MHz, RAM 2GB per core, and Giga-bit Ethernet)

4.2.7. Modified UHF Antenna

The model was slightly modified to have the exact size instead of having all the elements. So we remove some of the antenna elements to meet the size required.
The operating frequency is changed to 430MHz. We have used dipoles with 0.47 λ length for all the antennas. The spacing between all the elements are half wave length.

TIDES Model of the Antenna

Fore/Aft Antenna

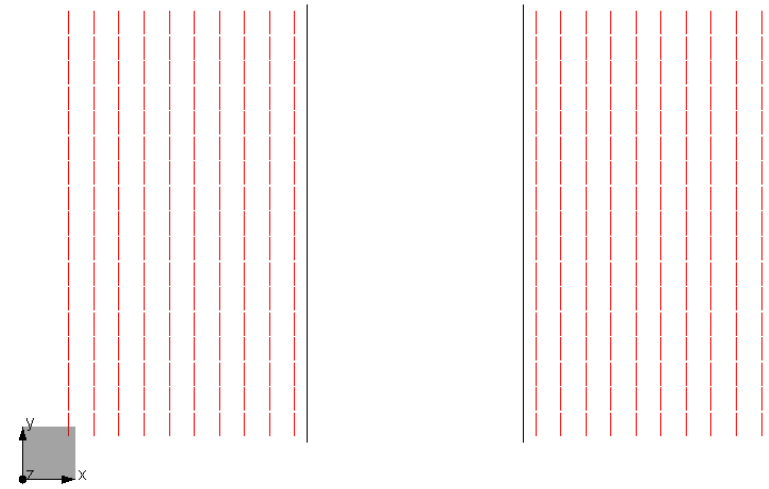

(a) Top view

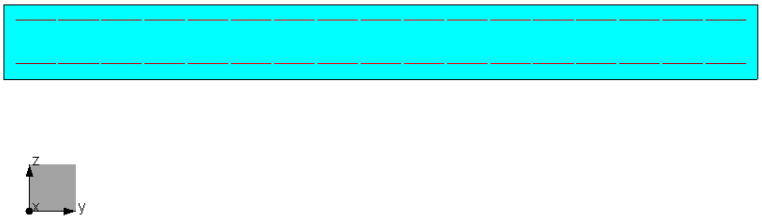

(b) Front view

Figure 20. (a) Top view and (b) Front view of Fore/Aft Antenna

The fore/aft antennas have 2 rows by 17 columns elements on each side of the structure. Totally, it has 34 elements on each side.

The size of the fore/aft antenna model is now 20 ft by 10.87 ft (depth).

The spacing between the director and the feeder is 1/4 λ, between the feeder and the reflector is also 1/4 λ, and between director and director is also 1/4 λ. The gain of the structure is shown in Fig. 21.

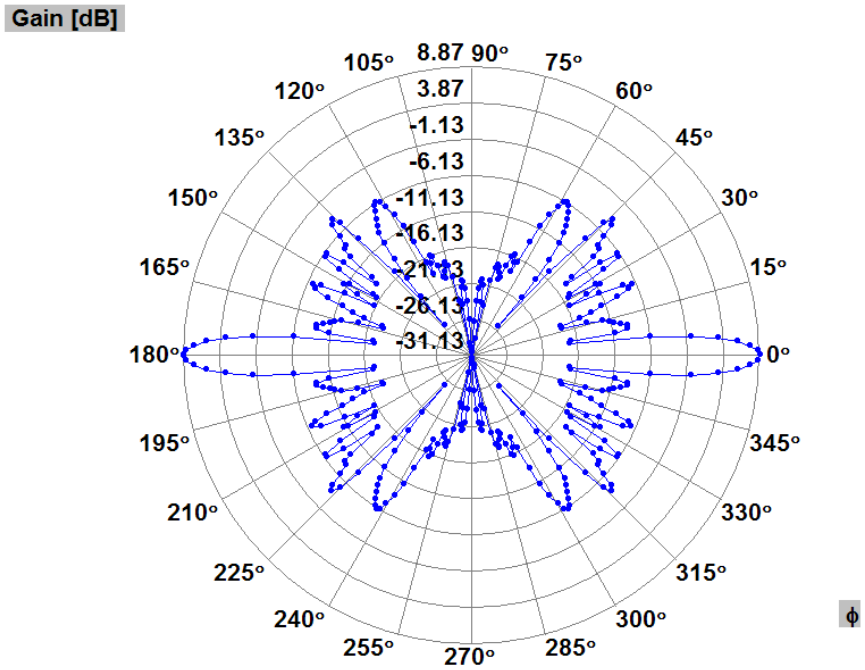

Figure 21. Azimuth Radiation Pattern for Fore/aft Antennas

The port/starboard antenna has 10 rows by 28 columns of antenna elements on each side. Totally, it has 280 elements on each side. The size of the Port/Starboard antenna model is 32 ft by 12 ft and is shown in Fig. 22. The gain of the antenna is shown in Fig. 23.

Port/Starboard Antenna

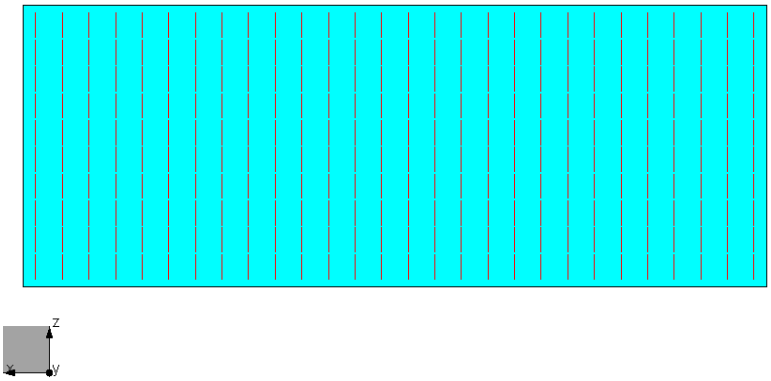

(a) Side view

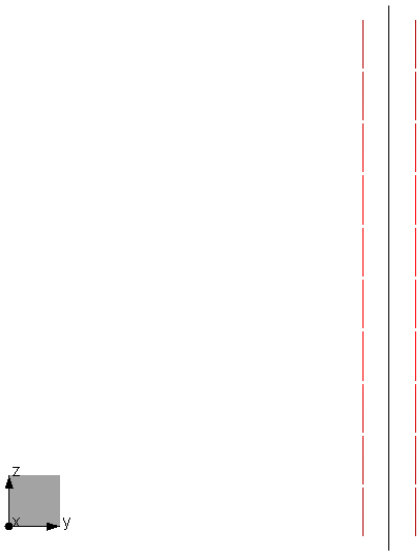

(b) Front view

Figure 22. (a) Side view and (b) Front view of Port/Starboard Antenna

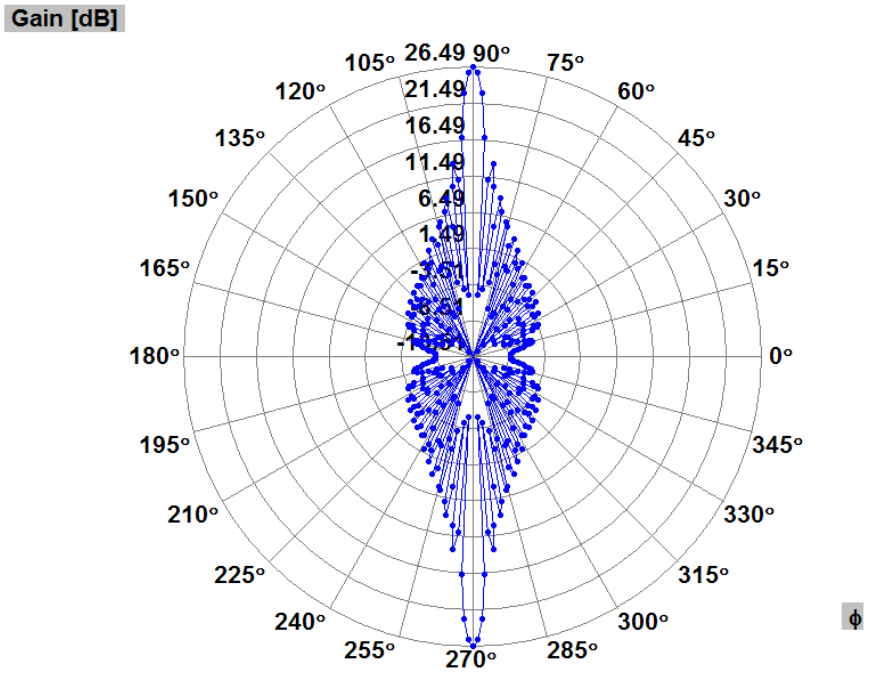

Figure 23. Azimuth Radiation Pattern for Port/starboard Antennas

4.2.7.1. TIDES Model of the Boeing 767 with Modified Antenna

We installed the “top hot” on to Boeing 767-200Era s shown in Fig. 24. The side views are shown in Fig. 25.

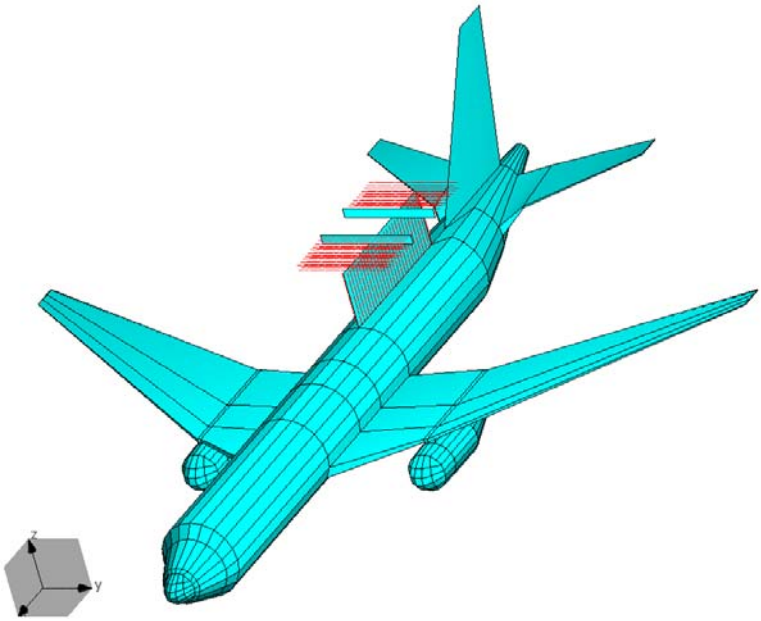

Figure 24. Boeing 767-200ER with the Antennas.

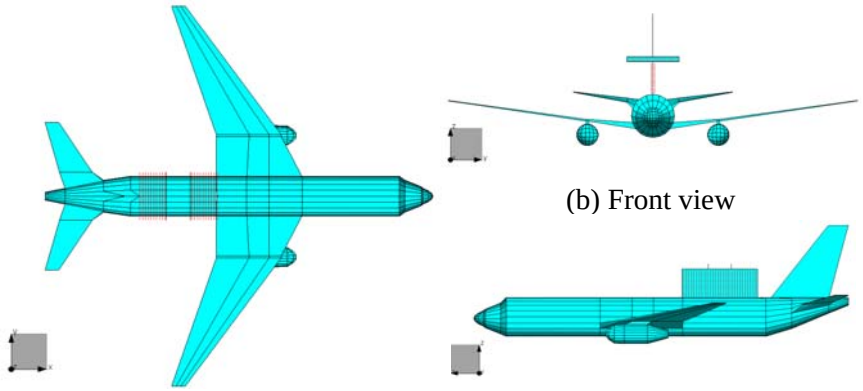

(a) Top view (b) Front view (c) Side view

Figure 25. (a) Top view, (b) Front view, and (c) Side view of Boeing 767-200ER with Antennas

4.2.7.2. Numerical Simulations and Results

Figure 26 shows the azimuth radiation pattern of the fore/aft and the port/starboard antennas in operating in free space along with the antennas mounted on the Boeing 767 - 200ER.

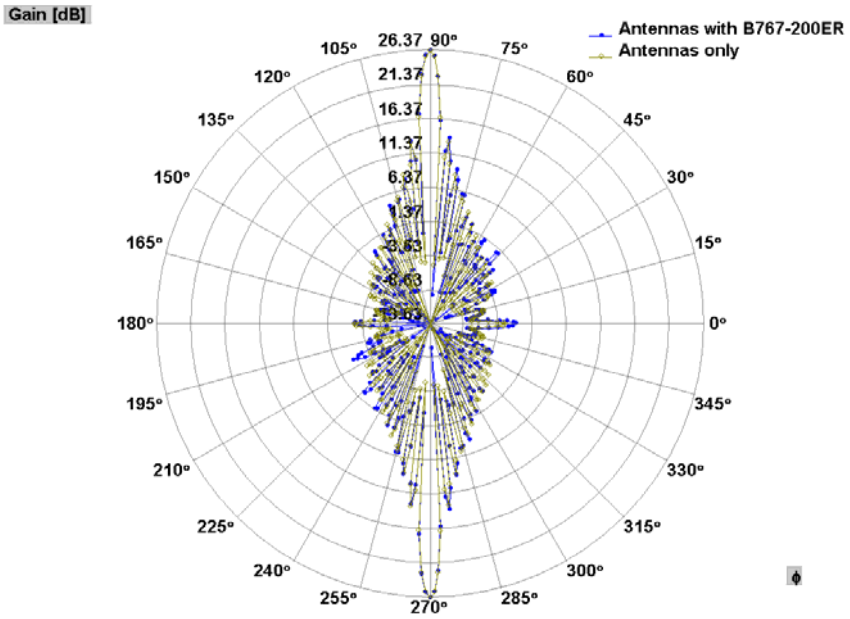

Figure 26. Azimuth Radiation pattern (Blue: Antennas with B767-200ER, Yellow: Antennas only

For the fore/aft antennas, we have 34 generators on each side and for the port/starboard antennas, we have 280 generators on each side. That's the reason why one plot shows more gain on the port/starboard antennas than on the fore/aft antennas. To zoom in only along the direction of Φ from 60° to 120°, we make finer steps from 60° to 120° to observe the pattern in details as shown in Figure 27.

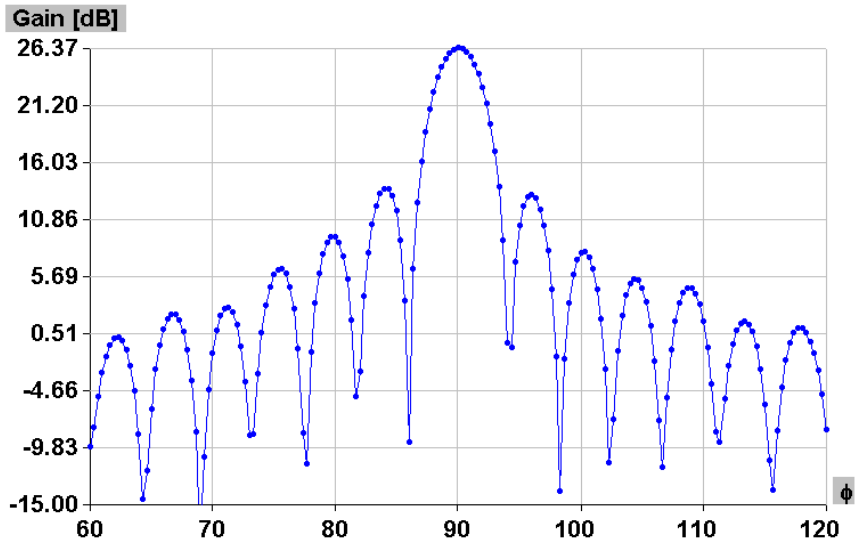

Figure 27. Azimuth Radiation pattern (From 60° to 120°)

The number of unknowns used in this simulation is 103777 at 430 MHz. This solution took about 410 minutes (about 6 Hours 50 mins) using the Parallel TIDES code on the CEMLAB Cluster. (4 nodes, 32cores, CPU speed 2.66MHz, RAM 2GB per core, and Giga-bit Ethernet).

5. CONCLUSIONS AND RECOMMENDATIONS

As we mentioned, fore/aft antennas have fewer generators than port/starboard antennas. We can put more weight on the excitations of the fore/aft antennas so as to balance the radiation from port/starboard antennas. One can in addition, optimize the antennas and meet the requirement like maximum gain along certain directions. Also one can focus further on enhancing the radiation along certain directions of interest. These are a few topics worth pursuing for further research.

Finally, it is important to merge the signal processing aspects with the electromagnetic analysis to obtain a complete representation of the entire system. As in any application, the response of the sensors needs to be deconvolved out in order to obtain an accurate representation of the solution. This is where the electromagnetic analysis becomes important. Unless the sensors effects and the effect of the platform are factored out just performing signal processing does not produce anything useful. The final objective in all research will be to merge the electromagnetic analysis with the signal processing methodology which this report has illustrated in a succinct way.

6. REFERENCES

[1] Wikipedia, Boeing 737 AEW&C, http://en.wikipedia.org/wiki/Wedgetail

[2] Northrop Grumman, 737 Airborne Early Warning & Control System (AEW&C), http://www.es.northropgrumman.com/solutions/737aewc/index.html

[3] Northrop Grumman, Multi-Role Electronically Scanned Array (MESA) Surveillance Radar (Video), http://www.es.northropgrumman.com/solutions/mesa/index.html

[4] Airforce-technology, 737 AEW&C Wedgetail Airborne Early Warning and Control Aircraft, USA, http://www.airforce-technology.com/projects/737aewc/

[5] Wikipedia, Boeing 767, http://en.wikipedia.org/wiki/Boeing_767

[6] Boeing, 767 Family, http://www.boeing.com/commercial/767family/specs.html

[7] Antennas 2nd edition, John D. Kraus, McGraw-Hill Book Company

7. LIST OF ACRONYMS

AEW&C	Airborne Early Warning and Control
CPU	Central Processing Unit
FMMT	Fourier-Modified Mellin Transform
MESA	Multi-role Electronically Scanned Array
MHz	Megahertz
MMT	Modified Mellin Transform
MT	Mellin Transform
RAAF	Royal Australian Air Force
RAM	Random Access Memory
RF	Radio Frequency
P1	Polyphase Code 1
P2	Polyphase Code 2
P3	Polyphase Code 3
P4	Polyphase Code 4
TIDES	Target IDEntification Software
UHF	Ultra High Frequency